# Modeling of coagulation and dispersion of aerosolsin the atmosphere

A.T. Celada and A. Salcido
*Instituto de Investigaciones Eléctricas, Gerencia Sistemas de Calidad, Ambiente y Seguridad,*
*Reforma 113, Col. Palmira, 62490 Cuernavaca, Morelos, México,*
*e-mail: atcelada@iie.org.mx*

Recibido el 14 de mayo de 2008; aceptado el 4 de noviembre de 2008

A simple model to analyze the effects of coagulation and turbulent dispersion on the behaviour of atmospheric aerosols is proposed here. This model does not use the concept of monomeric structure for the aerosol particles as proposed by Smoluchowsky to describe the coagulation. Instead, a probabilistic estimate of the production rate of the aerosol particles that are created by coagulation is carried out in the model as a function of the diameter ranges of the particles that collide. Only collisions of two particles with preservation of mass and volume are taken into account, and it is assumed that coagulation always occurs. The dispersion process of the aerosol is implemented by means of a simple Monte Carlo approach, where the mass fluxes are estimated with the mean wind field and the distribution of the turbulent fluctuations of wind velocity. Coagulation and dispersion are coupled in the mathematical formulation and numerical solution of the mass balance equations of the model. With this model we studied the steady state behaviour of an aerosol released to the atmosphere by an elevated point source. In particular, we studied the way in which the processes of coagulation and dispersion affect the distribution of the particle number, and also their effects on the concentration of the number of particles as a function of the downwind distance from the emission source. Qualitatively, some results obtained, such as a very fast consumption of the smallest aerosol particles near the source, and the accumulation of larger particles at greater distances, are in agreement with documented experimental findings.

*Keywords:* Polydispersed aerosols; turbulent dispersion; Brownian coagulation; turbulent coagulation; mathematical modeling.

En este trabajo se presenta un modelo sencillo para el estudio de los efectos de los procesos de coagulación y dispersión turbulenta sobre el comportamiento de los aerosoles en la atmósfera. En este modelo, a diferencia de la teoría de Smoluchowsky, la descripción del proceso de coagulación no considera estructura monomérica alguna para las partículas del aerosol, sino que se realiza una estimación probabilista de la tasa de producción de las partículas por efecto de la coagulación, como función de los intervalos de diámetros a los que pertenecen las partículas involucradas en las colisiones. En el modelo se consideran solamente colisiones binarias que conservan la masa y el volumen del aerosol, y se supone también que la coagulación ocurre en toda colisión. Por su parte, el proceso de dispersión del aerosol en la atmósfera por efecto de la turbulencia se instrumenta en el modelo a través de un proceso de Monte Carlo sencillo en el que los flujos de masa se estiman mediante el campo de viento medio y la distribución de las fluctuaciones turbulentas de la velocidad del viento. Estos dos procesos, coagulación y dispersión, se introducen de manera acoplada en la formulación matemática y en la solución numérica de las ecuaciones de balance del modelo. En este trabajo usamos este modelo para estudiar el comportamiento en estado estacionario de un aerosol que es descargado a la atmósfera por una fuente puntual elevada. Los resultados obtenidos muestran los efectos de la coagulación sobre la concentración de número de partículas, y la distribución espacial del aerosol como una función de la distancia hacia donde el viento sopla. El consumo de las partículas más finas, cerca de la fuente de emisión, y la acumulación de partículas con diámetros entre 0.12 y 0.96 $\mu$m conforme el aerosol se aleja de la fuente de emisión, son algunos efectos que coinciden cualitativamente con evidencias experimentales ya reportadas en la literatura.

*Descriptores:* Aerosoles polidispersos; dispersión turbulenta; coagulación browniana; coagulación turbulenta; modelación matemática.

PACS: 82.70.Rr; 92.60.Mt; 92.60.Sz

## 1. Introduction

The increasing concentrations of aerosols in the atmosphere represent an environmental problem because they produce damages to human health, reduce the visibility in the atmosphere, modify the properties of clouds, and play an important role in climate change, among other adverse effects. A complete understanding of the aerosol interactions with the environment requires multidisciplinary studies involving theoretical and experimental methods in order to quantify their effects on the environment. This has led to the development of numerical models that simulate the processes of transport, dispersion and transformation of aerosols in the atmosphere and determine their chemical composition and size distribution. In general, aerosol transformation refers to chemical reactions, coagulation, condensation, evaporation, nucleation, and gravitational sedimentation [1]. Among these processes, coagulation is particularly important because it contributes to the aerosol size distribution and has an important influence on the mixing state of the aerosol components. Moreover, coagulation may be considered to be the main growing mechanism of the fine particles (with diameters ranging from 0.001 to 0.100 $\mu$m) [1,2]. Aerosol coagulation is a very relevant process in engineering areas where the processes depend on the particle size distribution (*e.g.* inkjet printing, painting, water treatment, etc.). Also, as a result of the fossil fuel combustion in industry and heat engines, fine and large particles are produced and emitted to the atmosphere in the residual gas of combustion, and the size distribution of these particles changes during the first few minutes after emission due to such growing mechanisms as coagulation [3].

Most of the models for the atmospheric dispersion of aerosols that have been reported in the literature take into account the aerosol processes through modifications of the Gaussian plume model [4,5] or through the numerical solution of some approximations derived from the Reynolds averages of the mass balance equations [6]. Nevertheless, the numerical approaches that ordinarily are used in these models give over-smoothed space–time distributions of the pollutant concentrations which in no way reflect the fluctuating and random character of the atmospheric turbulent dispersion [7,8]. On the other hand, in general these models do not consider coagulation in their estimations because it has a limited effect on the mass distribution of large particles [9-11]. However, the coagulation process plays a very significant role in the size distribution of fine particles in such a way that, when coagulation is neglected, the aerosol number densities become overestimated and a wrong estimation of the mass distribution among all the aerosol particles results, even if the total mass of the aerosol is calculated adequately [12]. Moreover, the atmospheric aerosols had a polydisperse nature in general, and the coagulation theory of Smoluchowsky, which is the basis of many applications both theoretical and experimental [1,2,13], cannot be used to estimate properly the atmospheric aerosol coagulation because it deals only with aerosols that have a monomer structure. In order to overcome this limitation, in 1994 Jacobson [14] extended the application of the Smoluchowsky theory by introducing the concept of volume fraction $f_{ijk}$ to distribute the volume of particles formed by coagulation between the intervals of adjacent sizes in the monomer description; and Celada and Salcido in 2003 [15-17], on the other hand, proposed a statistical estimate of polydisperse coagulation based on the probability $Q^{\gamma}_{\alpha\beta g}$ that the collision between particles of bins $\boldsymbol{ß}_\alpha$ and $\boldsymbol{ß}_\beta$ will produce a new particle with a diameter in some other bin $\boldsymbol{ß}_\gamma$.

In this work, we propose a very simple mean field model for coagulation and atmospheric dispersion of polydisperse aerosols. In this model, the air-aerosol system is contained in a spatial region inside of which the aerosol processes such as emission, transport, dispersion and coagulation may take place. This spatial region is modeled as a 3D lattice of cells, each one of them being considered an open reactor that can exchange aerosol particles (because of the wind) with its first nearest neighbors. In this model, the mean wind field and the distribution function of the turbulent fluctuations in the wind velocity are assumed to be known, and the mass fluxes between adjacent cells are estimated from them using a Monte Carlo simulation approach as described by Salcido *et al*. [7,18-20]. Furthermore, inside each reactor-cell the aerosol size distribution may change due to the coagulation of its particles. The aerosol coagulation is estimated with the mean field coagulation model proposed by Celada and Salcido for polydisperse aerosols [15-17]. All the lattice cells of the simulation domain are updated in parallel according to the mass balance equations for each time step.

The aerosol coagulation-dispersion model was used to simulate the behavior of an aerosol released to the atmosphere by an elevated point source and to analyze the effects of the coagulation and dispersion processes on the space-time distribution of the number concentrations. The spatial distribution of the number concentration was studied as a function of the downwind distance from the emission source. The effects of coagulation can be summarized as a significant reduction in the number concentrations of the finest aerosol particles near the emission source, and the accumulation of particles with diameters between 0.12 and 0.96 $\mu$m, at greater distances. Qualitatively, the aerosol behavior we observed in the simulations is in agreement with the experimental observations by Zhu *et al*., [21,22] and Weijers *et al.* [23] with aerosols of traffic emissions.

## 2. Formulation

Let us consider a number $N$ of air pollution point sources, located at points $\mathbf{x}_s$ (*s = 1,*... , *N*) inside the spatial domain of interest, S. Each one of these sources discharges the same $\Lambda$ different pollutant species into the atmosphere, and the emission rate for the species $\alpha$ ($\alpha$ = 1, ... $\Lambda$) will be denoted by $Q_\alpha(\mathbf{x}_s, t)$ for the source located at $\boldsymbol{x}_s$. The pollutants' motion in the atmosphere is assumed to be governed by their advection caused by the wind field $\boldsymbol{v}(\boldsymbol{x}, t)$, which will be expressed as the mean wind field $\boldsymbol{u}(\boldsymbol{x}, t)$ plus a fluctuation term $\boldsymbol{w}(\boldsymbol{x}, t)$. We assume also that the turbulent component $\boldsymbol{w}(\boldsymbol{x}, t)$ can be computed from the probability density function $F(\boldsymbol{w}, t)$ of the turbulent fluctuations in the wind velocity by a Monte Carlo process. Here, $F(\boldsymbol{w}, t)d^3\boldsymbol{w}$ is the probability that one wind velocity turbulent fluctuation will have its value between $\boldsymbol{w}$ and $\boldsymbol{w} + d\boldsymbol{w}$. The probability density $F(\boldsymbol{w}, t)$ depends on the state of the atmospheric turbulence, and we assumed that it can be calculated for any given turbulence scenario from the experimental data.

For any simply connected region, $R$, located inside the spatial domain $S$, the mass conservation principle, applied to the mass transport phenomenon of the pollutant species $\alpha$, can be expressed as the well-known eulerian mass balance equation

$$\frac{d}{dt}\int_R \mu_\alpha(\mathbf{x}, t)\, dV = -\oint_{\partial R} \mathbf{J}_\alpha(\mathbf{x}, t)\, \cdot\, \mathbf{n}\, dA$$
$$+ \sum_s \int_R Q_\alpha(\mathbf{x}, t)\, \delta(\mathbf{x} - \mathbf{x}_s)\, dv + \int_R r_\alpha(\mathbf{x}, t)\, dV \qquad (1)$$

where $\partial R$ denotes the boundary surface of the region $R$, $\mu_\alpha(\mathbf{x}, t)$ is the mass density of the pollutant, $\mathbf{J}_\alpha(\mathbf{x},t) = \mu_\alpha(\mathbf{x},t)\mathbf{v}(\mathbf{x},t)$ is its mass flux vector, and $r_\alpha$ is the production rate of this pollutant due to its physical and chemical transformations in the atmosphere.

Now, let $\{C_i\}$ denote one finite discrete partition of the spatial domain S, composed of $M$ rectangular cells $C_i$ (i = 1,... , $M$) with the same linear dimensions *Lx*, *Ly* and

*Lz*. For each cell $C_i$, the volume average of any intensive property $F(\mathbf{x},t)$ is given by

$$\langle F(\mathbf{r}_i,t)\rangle \;=\; \frac{1}{V}\int\limits_{C_i}(F(\mathbf{x},t)\,dV \tag{2}$$

where $\boldsymbol{r}_i$ denotes the position of the cell (defined by its geometric center), and $V$ denotes its volume. In terms of cell averages, the mass balance equation for the cell $C_i$ can be expressed as

$$\frac{d}{dt}\int\limits_{R}\langle\mu_\alpha(\mathbf{r}_i,t)\rangle = \;\phi_\alpha(\mathbf{r}_i,t) + \sum_s \langle Q_\alpha(\mathbf{x}_s,t)\rangle\,\delta(\mathbf{x}_s,\mathbf{r}_i) + \langle r_\alpha(\mathbf{r}_i,t)\rangle \tag{3}$$

where $\delta(\mathbf{x}_s,\boldsymbol{r}_i)$ is equal to 1 if $\mathbf{x}_s$ defines a point inside of the cell $C_i$ and equal to 0 otherwise, and

$$\phi_\alpha(\mathbf{r}_i,t) \;=\; -\frac{1}{V}\oint\limits_{\partial C_i}\mathbf{J}_\alpha(\mathbf{x},t)\cdot\mathbf{n}dA \tag{4}$$

denotes the pollutant mass exchange rate (per volume unit) of the cell $C_i$ with its neighbors through its boundary surface $\partial C_i$.

If only interactions up to first nearest neighbors are assumed, the mass exchange rate $\Phi_\alpha(\boldsymbol{r}_i,t)$ can be modeled in terms of the cell-average values of the mass density and wind velocity in the cell $C_i$ and its six first neighboring cells, as follows:

$$\phi_\alpha(\mathbf{r}_i,t) \;=\phi_\alpha^{input}(\mathbf{r}_i,t) \;-\; \phi_\alpha^{output}(\mathbf{r}_i,t) \tag{5}$$

where

$$\phi_\alpha^{output}(\mathbf{r}_i,t) = \langle\mu_\alpha(\mathbf{r}_i,t)\rangle\left\{\frac{|v_x(\mathbf{r}_i,t)|}{L_x} \;+\; \frac{|v_y(\mathbf{r}_i,t)|}{L_y} \;+\; \frac{|v_z(\mathbf{r}_i,t)|}{L_z}\right\} \tag{6}$$

$$\phi_\alpha^{input}(\mathbf{r}_i,t) = \frac{1}{2}\sum_{k=1}^{3}\times\frac{1}{L_k}\left\{\langle\mu_\alpha(\mathbf{p}_k,t)\rangle\left[|v_k(\mathbf{p}_k,t)\,|+v_k(\mathbf{p}_k,t)\,\right] \;+\; \langle\mu_\alpha(\mathbf{q}_k,t)\rangle\left[\,|v_k(\mathbf{q}_k,t)\,|+v_k(\mathbf{q}_k,t)\right]\right\} \tag{7}$$

with

$$\mathbf{p}_k \;=\; \mathbf{r}_i \;-\; \mathbf{e}_k L_k \qquad\qquad \mathbf{q}_k \;=\; \mathbf{r}_i \;+\; \mathbf{e}_k L_k \tag{8}$$

where $\mathbf{e}_k$ (k = 1,2,3) are the unit vectors along the coordinate axis, and $v_k$ are the cell-averages of the wind velocity components.

Within this modeling framework, the cell-average of the mass density of the pollutant $\alpha$ in the cell $C_i$, at time $t+\delta t$, can be computed as follows:

$$\langle\mu_\alpha(\mathbf{r}_i,t{+}\delta t\rangle = \langle\mu_\alpha(\mathbf{r}_i,t)\rangle + \delta t\left\{\phi_\alpha(\mathbf{r}_i,t){+}\sum_s\langle Q_\alpha(\mathbf{x}_s,t)\rangle\,\delta(\mathbf{x}_s,r_i){+}\langle r_\alpha(\mathbf{r}_i,t)\rangle\right\} \tag{9}$$

Nevertheless, the model with interactions up to the first nearest neighbors calls for the mass exchange rate [defined by Eqs. (5), (6), and (7)], an integration time step $\delta t$ which does not exceed the eulerian time scale $\tau$ defined by

$$\tau \;=\; \frac{1}{2}\left(\frac{L_x\,L_y\,L_z}{L_y\,L_z\,|V_{x_{\max}}| \;+\; L_x\,L_z\,|V_{y_{\max}}| \;+\; L_x\,L_y\,|V_{z_{\max}}|}\right) \tag{10}$$

where $|V_{xmax}|$, $|V_{ymax}|$ and $|V_{zmax}|$ denote the upper bounds to the wind velocity components in the X, Y, and Z directions.

The influence of atmospheric turbulence on the pollutants' dispersion process is represented in this model through the turbulent fluctuation component **w** of wind velocity **v.** At each cell $C_i$ of the simulation spatial domain $S$, the cell-average of wind velocity can be expressed as:

$$\mathbf{v}(\mathbf{x}_i,t) \;=\; \mathbf{u}(\mathbf{x}_i,t) \;+\; \mathbf{w}(\mathbf{x}_i,t) \tag{11}$$

where $\mathbf{u}(\boldsymbol{x}_i,t)$ is the mean wind vector in the cell. The turbulent component **w** can be computed through a Monte Carlo process once the probability density function F($\boldsymbol{w},t$) is known. In the computer simulations, for each cell $C_i$ and any given time $t$, a randomly selected value $\boldsymbol{p}$ of the probability density F($\boldsymbol{w},t$) (as estimated from wind velocity measurements for a given turbulence scenario) will define (depending on the particular statistics of the turbulent fluctuations) a small set of fluctuation values $\{\boldsymbol{w}_n\}$**,** and one of them can be selected randomly to fix the wind velocity. This Monte Carlo estimation process, however, requires knowledge of the mean wind field $\mathbf{u}(\boldsymbol{x}_i,t)$, and of the probability density F($\boldsymbol{w},t$) at each cell $C_i$ of the simulation spatial domain $S$.

The probability density F($\boldsymbol{w},t$) may be estimated from wind velocity measurements carried out with fast 3D

anemometers. For example, in Fig. 1 we present measurements of the wind velocity x-component ($\mathbf{v}_x$) and their 1-minute averages ($\mathbf{u}_x$), for the 01:00 – 02:00 hour period (local time), obtained with an ultrasonic 3D anemometer, on March 15, 2001, in the southern part of Mexico City. These data were obtained during a micrometeorological campaign carried out in the Mexico City Metropolitan Area (MCMA) by the Instituto de Investigaciones Eléctricas (IIE) with support from the National Council of Science and Technology (CONACYT) [24]. For the purposes of this campaign, three micrometeorological surface stations were installed at sites located in the North (Azcapotzalco site, 19°30'09.4" N, 99°11'12.2" W, 2190 masl), Northeast (Texcoco site, 19°27'53.1" N, 98°59' 54.4" W, 2250 masl) and South (Xochimilco site, 19°18'18.3" N, 99°06'6.2" W, 2250 masl) of the MCMA. Each station was equipped with a 3D ultrasonic turbulence sensor and with conventional meteorological sensors for temperature, relative humidity, pressure, global radiation, net radiation, and precipitation. The sampling rates were 10 Hz for the ultrasonic sensor and 1 Hz for the conventional sensors. One-hour averages were calculated for all the meteorological parameters and for turbulence parameters such as friction velocity, scale temperature, Monin-Obukhov length, sensible heat flux, and turbulent kinetic energy, among others. Additional information about the campaign and the micrometeorological data can be found at www.geocities.com/mexicomdb.

In Fig. 2, the probability density of the wind velocity turbulent fluctuations $\mathrm{w}_x$ around the 1-minute averages is shown for the same case. As can be observed, the distribution of the turbulent fluctuations presents a Gaussian behavior as a result of a fully developed state of atmospheric turbulence. This behaviour, however, changes throughout the day and the turbulent fluctuations can have different distributions, as presented in Fig. 3 for the experimental data obtained on April 1, 2001, in the same micrometeorological campaign.

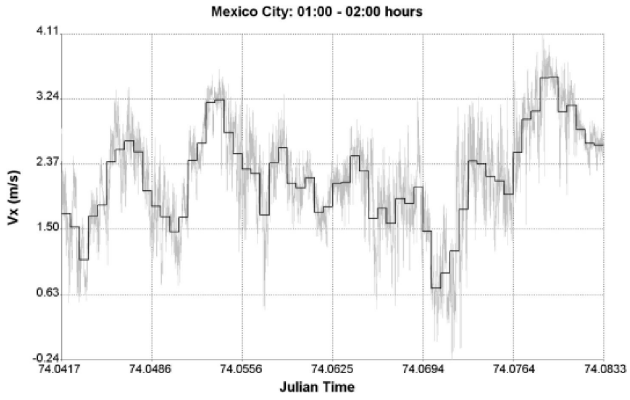


FIGURE 1. Wind velocity x-component (gray line) and its 1-minute average (black staggered line) for the 01:00 – 02:00 time period of March 15, 2001, at a micrometeorological station located in the southern part of Mexico City [24].


FIGURE 2. Distribution of the turbulent fluctuations of the wind velocity x-component around the 1-minute average for the 01:00 – 02:00 time period of March 15, 2001, at a micrometeorological station located in the southern part of Mexico City [24].

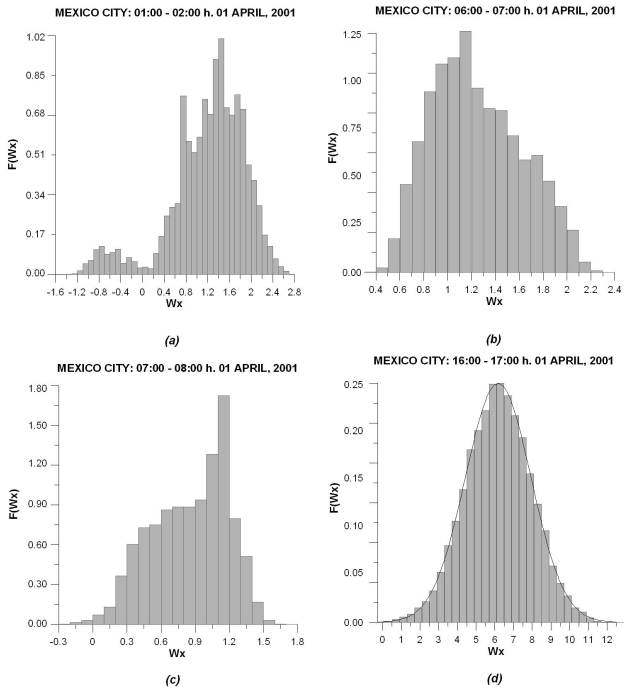


FIGURE 3. Distributions of the turbulent fluctuations of the wind velocity x-component around the 1-minute average for the a) 01:00 – 02:00 h, b) 06:00 – 07:00 h, c) 07:00 – 08:00 h, d) 16:00 – 17:00 h, on April 1, 2001, at one micrometeorological station located at Xochimilco [24].

The production rates $\langle r_\alpha \rangle$ are related to the physical and chemical transformations of the pollutants in the atmosphere and they represent the mass pollutants' sources and sinks. Estimating the pollutants' production rates comprises, in general, a very complex problem. In this paper, however, we shall be concerned only with the production of aerosol particles by coagulation processes.

In two recent works, we proposed a simple mean field coagulation model for polydisperse aerosols [15,16]. This model (hereafter referred to as MFC), as does the Smoluchowsky coagulation theory, considers an aerosol made up of

spherical particles that coagulate each time they collide and participate only in binary collisions that preserve the mass and volume of the aerosol. In the MFC model, however, an aerosol particle is not considered to be composed of an integral number of monomers; instead, the aerosol size spectrum is divided into a given number $\Omega$ of non-overlapping diameter intervals (or bins) $\mathbf{ß}_\alpha$ withg different lengths in general, and the size distribution is described in terms of the $\Omega$ number densities $n_\alpha$ of the aerosol particles contained in the intervals $\mathbf{ß}_\alpha$. Thus the aerosol has a polydisperse nature in this model.

Besides, the coagulation dynamics depends not only on the concentrations of the particles in the bins, and on the collision frequency (as described by a coagulation kernel), but also on the probability $Q^\gamma_{\alpha\beta}$ that the collision between particles of the bins $\mathbf{ß}_\alpha$ and $\mathbf{ß}_\beta$ will produce a new particle with diameter in some other bin $\mathbf{ß}_\gamma$. When a collision takes place in the system, it may involve one particle of some bin $\mathbf{ß}_\alpha$ and another one of some bin $\mathbf{ß}_\beta$ with a probability $P_{\alpha\beta}$ which depends on the particular collision driving mechanism (brownian motion, turbulence, or some other) and on the values of the aerosol number densities $n_\alpha$ and $n_\beta$ in these bins. These particles will coagulate, producing a new aerosol particle which may belong to one of the bins $\mathbf{ß}_\alpha$ and $\mathbf{ß}_\beta$, or to some other bin $\mathbf{ß}_\gamma$ depending on its volume (which must be equal to the sum of the volumes of the incident particles). This will occur with some probability $Q^\gamma_{\alpha\beta}$. So, the mass production rate of the aerosol particles in bin $\mathbf{ß}_\gamma$ may be expressed as:

$$r_\gamma \;=\; \frac{1}{2}\sum_{\alpha,\beta\neq\gamma}^{\Omega} P_{\alpha_\beta} Q^\gamma_{\alpha\beta} \;-\; \sum_{\alpha,\beta=1}^{\Omega} P_{\alpha\beta}\,(1 \;-\; Q^\gamma_{\alpha\beta}) \quad (12)$$

where the first term on the right-hand side represents the particles created in $\mathbf{ß}_\gamma$ by the collisions of the particles belonging to all other bins different from $\mathbf{ß}_\gamma$, while the second one represents the particles of the same kind consumed by their collisions with particles belonging to other bins. This equation does not, of course, take into account any effect of particle loss through mechanisms such as wall adhesion or others. The probability factor $P_{\alpha\beta}$ can be expressed as:

$$P_{\alpha\beta}{=}K(r_\alpha, D_\alpha, r_\beta, D_\beta, \ldots)\begin{cases} n_\alpha n_\beta & \text{if}\alpha=\beta \\ 2n_\alpha n_\beta & \text{if}\alpha\neq\beta \end{cases} \quad (13)$$

where $n_\alpha$ and $n_\beta$ are the number densities of particles in $\mathbf{ß}_\alpha$ and $\mathbf{ß}_\beta$, respectively, and $K$ is a proper coagulation kernel determined by the particular collision driving mechanism. The kernel $K$ will be a function of the incident particles' properties, such as their mean radii $r_\alpha$ and $r_\beta$ and their mean brownian diffusion coefficients $D_\alpha$ and $D_\beta$, and some other characteristics of the motion regime of the gas in which the particles are suspended, such as turbulence.

The probability factor $Q^\gamma_{\alpha\beta\mathrm{g}}$ takes into account the polydisperse nature of the aerosol, and it is related to the volume conservation when the particles collide. It might be possible to find out this probability experimentally; however, for purposes of this work it was estimated numerically as follows. For each triplet ($\mathbf{ß}_\alpha$, $\mathbf{ß}_\beta$, $\mathbf{ß}_\gamma$), the particle radii $r_\alpha$ and $r_\beta$ were made to run over the corresponding bins, and the respective particle volumes $V_\alpha$ and $V_\beta$ were calculated for each case. As it was assumed that coagulation preserves volume, the volume of the new particle is $V = V_\alpha + V_\beta$. Then, each time $V$ matched the radius of a particle in $\mathbf{ß}_\gamma$, a counter $q^{\gamma\mathrm{g}}_{\alpha\beta\mathrm{g}}$as increased by one. Finally, the probability $Q^\gamma_{\alpha\beta\mathrm{g}}$ was estimated by dividing the counter by the total number of cases. In the computer implementation of the MFC model, the probability $Q^\gamma_{\alpha\beta\mathrm{g}}$ is implemented as a lookup table. The inclusion of the polydisperse nature of the aerosol through the probability $Q^\gamma_{\alpha\beta\mathrm{g}}$ in the theoretical formulation of the model constitutes one of the main differences between the MFC model and others based on the Smoluchowsky theory.

In order to reflect the polydispersed nature of the aerosol and to conserve the aerosol volume, in 1994, Jacobson [14] extended the application of the Smoluchowsky theory to the simulation of particles with volumes which are not multiples of that of the monomer by introducing the concept of volume fraction $f_{ijk}$.This fraction is utilized to distribute the volume of the particles formed by coagulation between the intervals of adjacent sizes [25]. An important conceptual difference exists between Jacobson's model and our approach: in Jacobson's model, the fraction $f_{ijk}$ represents a distribution criterion of the particle volume formed by coagulation among adjacent size intervals, and it is introduced as an element that makes it possible to keep the monomeric concept of the Smoluchowsky theory for numerical estimates of coagulation of polydispersed aerosols. In the MFC model, on the other hand, the probability $Q^\gamma_{\alpha\beta\mathrm{g}}$ has a very clear physical meaning within the formulation context of the model [15-17]: it represents the probability of the creation of one particle in the diameter interval $\mathbf{ß}_\gamma$ as a result of the collision of particles that belong to the diameter intervals $\mathbf{ß}_\alpha$ and $\mathbf{ß}_\beta$.

In previous works [15,16,26], we showed that the MFC model could reproduce the brownian and turbulent coagulation experimental data already reported in the literature by Kim *et al*. [27], Rooker and Davies [28], and Okuyama *et al*. [29]. For brownian coagulation, we considered the brownian coagulation kernel [2]

$$K_B \;=\; 4\pi(r_\alpha \;+\; r_\beta)\,(D_\alpha \;+\; D_\beta) \quad (14)$$

where the particle radii $r_\alpha$ and $r_\beta$ were interpreted as their respective mean values in $\mathbf{ß}_\alpha$ and $\mathbf{ß}_\beta$, and the diffusion coefficients $D_\alpha$ and $D_\beta$ matching these mean radii were used. For brownian coagulation under turbulent conditions, the coagulation kernel was considered as the superposition

$$K_{BT} \;=\; K_B \;+\; K_T \quad (15)$$

of the Brownian kernel $K_B$ and the kernel $K_T$ drawn by Kruis and Kusters [30] to represent the effect of turbulence on coagulation:

$$K_T \;=\; \varepsilon_c \left(\frac{8\pi}{3}\right)^{1/2} (r_\alpha \;+\; r_\beta)^2 \left(w_a^2 \;+\; w_c^2\right)^{1/2} \quad (16)$$

where $r_\alpha$g and $r_\beta$, as above, are interpreted as the mean radii in $\mathbf{ß}_\alpha$ and $\mathbf{ß}_\beta$, and $w_a$ and $w_c$ are the particle relative velocities due to inertial and shear turbulent effects; $\varepsilon_c$ is an empirical coefficient (with values ranging from 1 to 3.5) introduced by Celada and Salcido [15-17] to modulate the collision efficiency.

## 3. Simulation results

Numerical simulations were performed to study the dispersion and coagulation processes of an aerosol emitted by a power plant. The aerosol size distribution and number concentrations were analyzed as functions of space and time under several conditions of emission, coagulation, and atmospheric dispersion.

For the simulations, the emission and meteorological scenarios were adopted from Buckholtz' work [4]. Here the emission source was a power plant of 750 MW (located in a flat, arid area covered by bushes) using coal as fuel. The aerosols emitted were composed mainly of aluminosilicates with a diameter range from 0.01 to 61.44 $\mu$m, and with a bimodal size distribution with maximum values of the number concentrations in the particle diameters of 0.03 and 0.96 $\mu$m. The aerosol dispersion took place on a clear, sunny day under meteorological conditions defined by a wind speed of 2.10 m/s and Pasquill stability class A. The velocity and temperature of the emissions were 16.76 m/s and 393.15 K, respectively. In Table I, a summary of the general characteristics of the emission source, characteristics of the aerosol emissions, and meteorological conditions is presented.

TABLE I. General characteristics of the emission source, aerosol emission and meteorological conditions [4].

| | |
|---|---|
| ***Characteristics of emission source*** | |
| *Emission source:* | Power Plant of 750 MW |
| *Stack diameter:* | 8.23 m |
| *Stack height :* | 76.20 m |
| *Combustible:* | Carbon |
| *Effluent temperature:* | 393.15 K |
| *Plume effective height:* | 483 m |
| ***Aerosol characteristics*** | |
| *Aerosol type* | Aluminosilicates |
| *Density* | 2.40 g/cm$^3$ |
| *Diameter range* | 0.01 – 61.44 $\mu$m |
| *Emission velocity of the aerosol* | 16.76 m/s |
| ***Meteorological conditions*** | |
| *Air temperature* | 283.15 K |
| *Atmospheric pressure* | 1 atm |
| *Mean wind speed* | 2.10 m/s |
| *Cloudiness* | Sunny day without clouds |
| *Atmospheric stability* | A class, Pasquill classification |
| *Relative humidity* | Low |

TABLE II. Diameter intervals and number concentration of particles in the emission source [4].

| *Diameter intervals* [$\mu$m] | *Mean diameter* [$\mu$m] | *Number Concentration* [# cm$^{-3}$] |
|---|---|---|
| $\beta_1$) 0.001 - 0.020 | 0.010 | $n_1$)52,613,299 |
| $\beta_2$) 0.020 - 0.040 | 0.030 | $n_2$) 415,573,785 |
| $\beta_3$) 0.040 - 0.080 | 0.060 | $n_3$) 362,914,064 |
| $\beta_4$) 0.080 - 0.160 | 0.120 | $n_4$) 34,255,783 |
| $\beta_5$) 0.160 - 0.320 | 0.240 | $n_5$) 731,952 |
| $\beta_6$) 0.320 - 0.640 | 0.480 | $n_6$) 973,484 |
| $\beta_7$) 0.640 - 1.280 | 0.960 | $n_7$) 1,134,797 |
| $\beta_8$)1.280 - 2.560 | 1.920 | $n_8$) 702,842 |
| $\beta_9$) 2.560 - 5.120 | 3.840 | $n_9$) 230,980 |
| $\beta_{10}$) 5.120 - 10.240 | 7.680 | $n_{10}$) 40,182 |
| $\beta_{11}$) 10.240 - 20.480 | 15.360 | $n_{11}$) 3,688 |
| $\beta_{12}$) 20.480 - 40.960 | 30.720 | $n_{12}$) 178 |
| $\beta_{13}$) 40.960 - 81.920 | 61.440 | $n_{13}$) 5 |

The plume rise and the topographic complexities of the terrain were not considered in the simulations. The mean wind field was considered uniform along the X-axis direction, and atmospheric turbulence was assumed to be homogeneous, isotropic and completely developed, which allowed us to use a Gaussian distribution function for the turbulent fluctuations. The aerosol size spectrum was divided into 13 diameter intervals $\beta_\alpha$, whose lower and upper bounds and number concentrations are described in Table II.

The values of the input parameters in the numerical simulations, such as the domain's spatial dimension, spatial and temporal resolutions ($\Delta$X$\Delta$Y$\Delta$Z and $\Delta$T), the initial conditions, the mean wind speed, and the standard deviations of the wind velocity components are included in Table III.

### 3.1. Effects of coagulation on the number concentration

In order to observe how the coagulation process affects the number concentration of nuclei ($< 0.12\mu$m), accumulation (0.12 $\mu$m $< d_p <$ 0.96 $\mu$m) and coarse particles (0.96 $\mu$m $< d_p <$ 7.68 $\mu$m), in Figs. 4 and 5 we present the time evolution of the number concentration up to the steady state condition, for cases with and without coagulation, respectively.

For the nuclei particles (diameters $<$ 0.12 $\mu$m), in the steady state condition, the number concentrations fell drastically. Particularly significant was the case of particles of 0.01 $\mu$m because the number concentrations decreased by 57% (see Fig. 4a). An important reduction in the nuclei particles has also been observed by Zhu *et al.* [21,22] for particles of traffic emissions with diameters smaller than 0.025 $\mu$m. They pointed out that this kind of particle reduced its concentration by about 25% in the nearest zones to the emission

source, and they concluded that the particle loss was a consequence of the coagulation process.

For particles with a diameter between 0.12 and 0.96 $\mu$m, the effect of coagulation on the number concentration was accumulation, as can be observed in Fig. 4b. Here the number concentration, in the steady state condition, is greater with coagulation than without coagulation. The particles growing from nuclei tend to accumulate in this mode, coagulating very slowly into larger particles. This accumulation of particles was also observed by Zhu *et al.*, [21,22] for vehicular emission particles with diameters close to 0.10 $\mu$m, which increased their number concentration at the same time that the aerosol moved far away from the emission source.

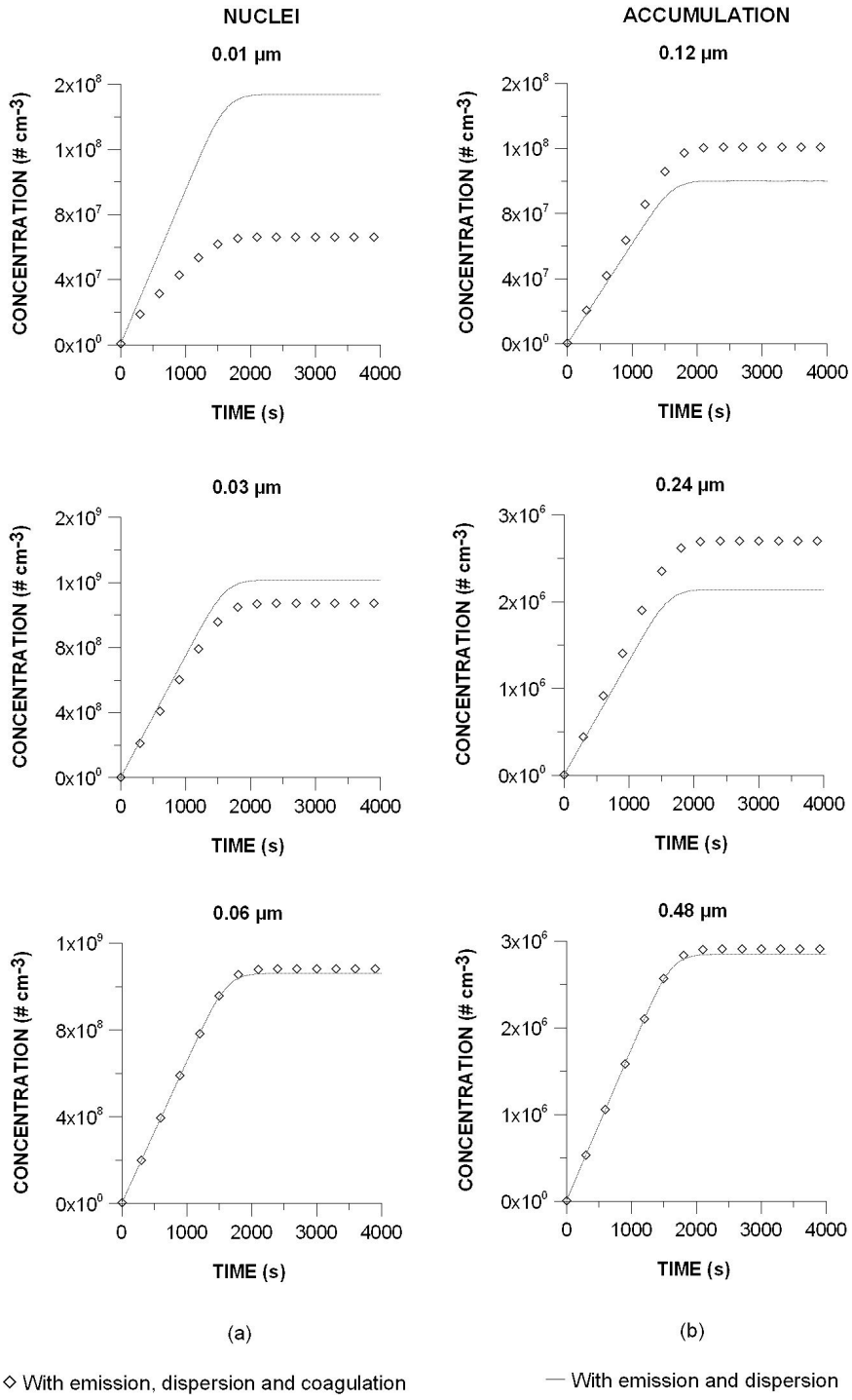


FIGURE 4. Aerosol number concentrations as a function of time for (a) nuclei and (b) accumulation particles with mean diameters from 0.01 to 0.48 $\mu$m. Simulation results obtained with the MFC model for the cases with and without coagulation.

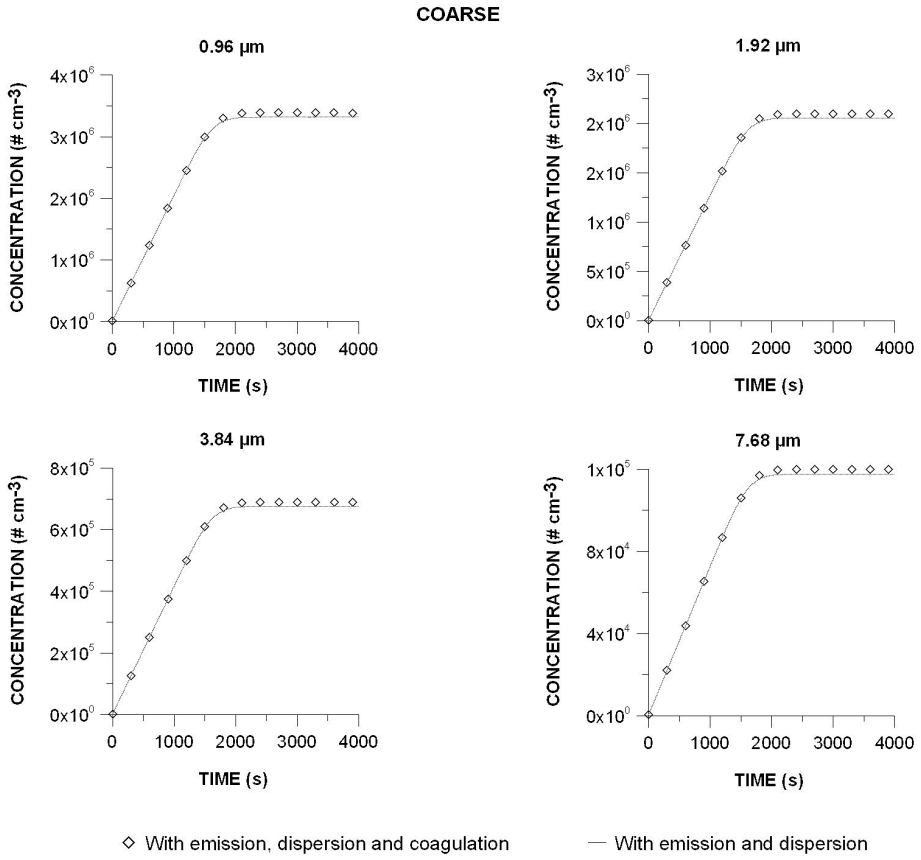


FIGURE 5. Aerosol Number concentrations as a function of time for coarse particles with diameters from 0.96 to 7.68 $\mu$m. Simulation results obtained with the MFC model for the cases with and without coagulation.

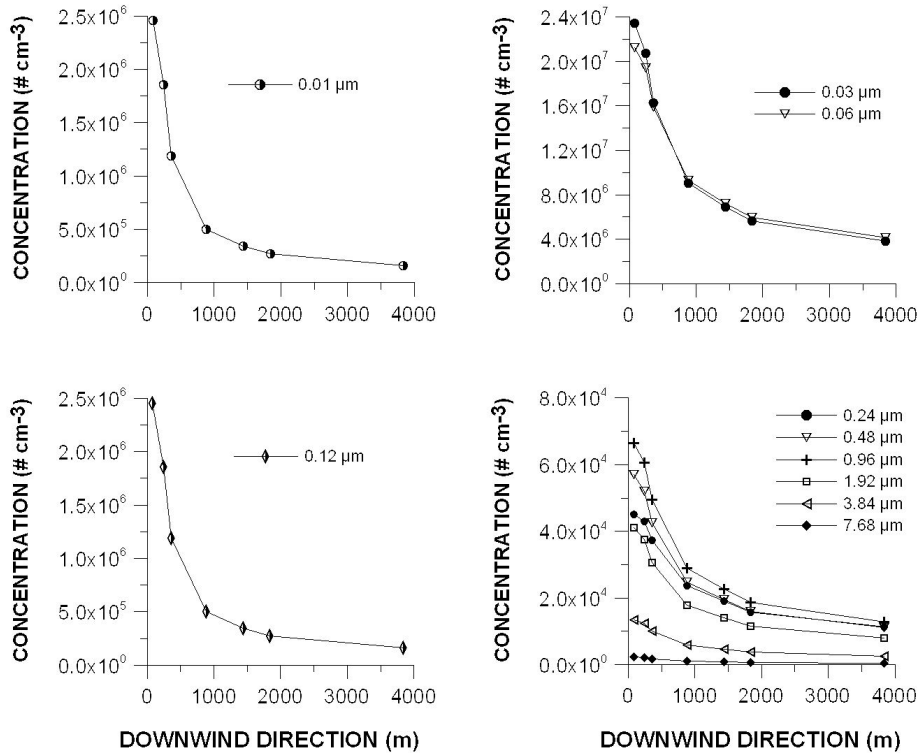


FIGURE 6. Aerosol number concentrations of particles with mean diameters from 0.01 to 7.68 $\mu$m as a function of downwind distance from the emission source. Simulation results obtained with the MFC model.

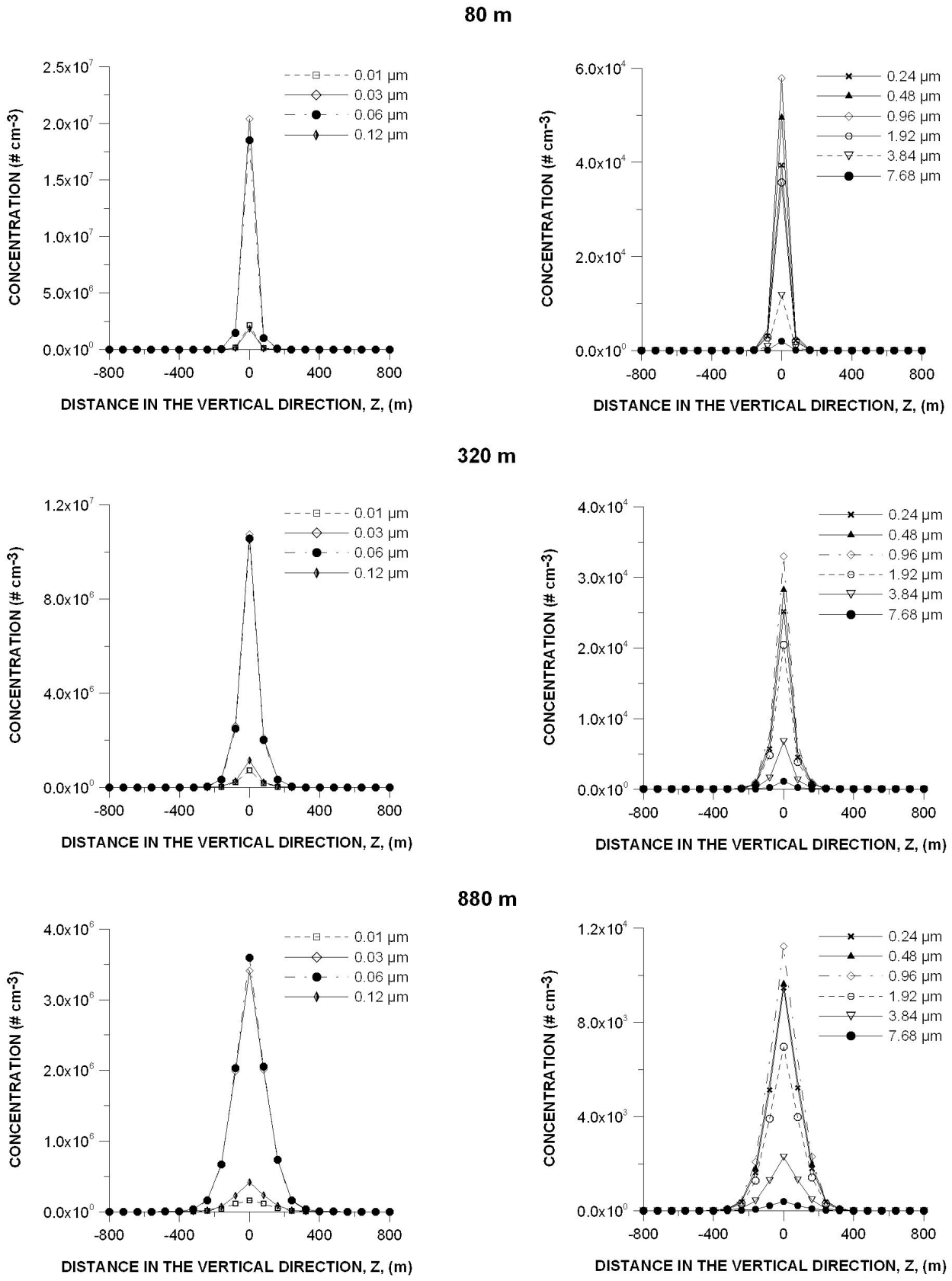


FIGURE 7. Steady state vertical distribution of number concentrations at downwind distances of 80, 320 and 880 m from the emission source. Simulation results obtained with MFC model.

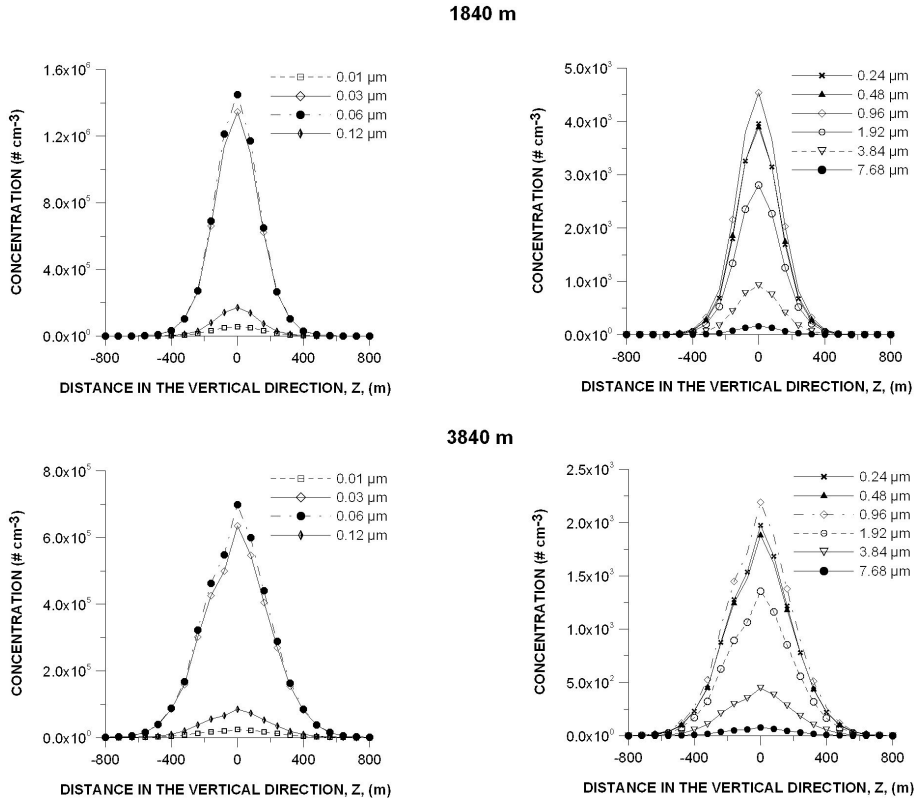


FIGURE 8. Steady state vertical distribution of number concentrations at downwind distances of 1840 and 3840 m from the emission source. Simulation results obtained with MFC model.

TABLE III. Input parameters used in the simulations.

| | |
|---|---|
| ***Spatial domain*** | |
| *X direction:* | 4000 m |
| *Y direction:* | 2400 m |
| *Z direction:* | 2400 m |
| ***Spatial resolution*** | |
| $\Delta X$ *:* | 80 m |
| $\Delta Y$ *:* | 80 m |
| $\Delta Z$ *:* | 80 m |
| ***Temporal resolution*** | |
| $\Delta t$*:* | 1 s |
| ***Initial conditions*** | |
| *Emission aerosol velocity:* | 16.76 m/s |
| ***Mean wind speed, wind speed standard deviations and turbulence intensity*** | |
| *Mean wind speed:* | 2.10 m/s |
| $\sigma_x$ : | 0.50 m/s |
| $\sigma_y$ : | 0.50 m/s |
| $\sigma_z$ : | 0.50 m/s |
| *Turbulence intensity :* | 0.24 |

For particles with larger diameters, the effects of coagulation in the simulations were reduced in such a way that particles with a diameter greater than 0.96 $\mu$m reached the same steady state concentration when the coagulation process was enabled than when it was not (see Fig. 5).

### 3.2. Number concentration as a function of distance from the emission source

The trend in the number concentrations for downwind distances from the emission source is shown in Fig. 6. Here, for all particle modes, a gradual decrease is observed in the number concentrations at large downwind distances. The most significant reduction was observed for particles with diameters around 0.01 $\mu$m. The concentration of these particles fell by 24% within the first 240 m from the emission source.

Similar results were found by Weijers *et al*. [23] for particles from traffic emissions with diameters smaller than 0.013 $\mu$m. They observed that the particle concentration was reduced by between 50 and 60% within the first 150 m from the emission source, and they suggested that, in the nuclei particles, the coagulation was more important than the atmospheric dilution.

In Figs. 7 and 8, the vertical distribution of the steady state number concentrations as a function of downwind distance from the emission source is presented for 80, 320, 880, 1840 and 3840 m.

## 4. Conclusions

A simple model was proposed for analyzing the effects of coagulation and atmospheric dispersion on the behavior of polydispersed aerosols. Coagulation is accomplished by including a probability function $Q^{\gamma}_{\alpha\beta g}$ to conserve the aerosol volume and to represent the different particle diameters in the aerosol. With this function we overcome the limitation of the Smoluchowsky theory in modeling the coagulation of particles with no monomeric structure. The aerosol dispersion in the atmosphere was taken into account through a Monte Carlo process for the mass flow.

We used this model to perform numerical simulations of the aerosol steady state behavior around an elevated emission point source burning coal. The results of the simulations showed that coagulation has an important role in the decrease of number concentrations of particles and in the the change in size distribution at a distance away from the emission source. Furthermore, the simulation results present coagulation as the main mechanism in the decay of the number concentration of nuclei particles (diameters smaller than 0.12 $\mu$m), close to the emission source. In addition, the accumulation of particles with mean diameters between 0.12 and 0.96 $\mu$m was observed. Finally, in the coarse mode particles (diameters ¿ 0.96 $\mu$m) the coagulation influence is not perceptible. Qualitatively, these results are in agreement with those observed in 2003 by Weijers *et al*. [23] and by Zhu *et al*. in 2002 [21,22], with aerosols of traffic emissions on a motorway in Amsterdam and two highways in California, USA, respectively.


1. J.H. Seinfeld and S.N. Pandis, *Atmospheric Chemistry and Physics. From Air pollution to Climate Change* (John Wiley & Sons, Inc., E.U.A., 1998) p. 1326.
2. S.K. Friedlander, *Smoke, Dust and Haze. Fundamentals of Aerosol Dynamics*, 2a. ed. (Oxfod New York: Oxford University Press, Oxfod, UK, 2000)407.
3. E. Lipsky, C.O. Stanier, S.N. Pandis, and A.L. Robinson. *Energy & Fuels,* **16** (2002) 302.
4. H.T. Buckholtz, *Evolution of particulate emissions from a coal-fired power plant.* Ph D. Thesis, Lawrence Livermore National Laboratory, California University, E.U.A., (1980)167.
5. C.M. Sheih, *Atmos. Environ*., **11**(1977)1185.
6. A.E. Aloyan, V.O. Arutyunyan, A.A. Lushnikov, and V.A. Zagaynov, *J. Aerosol Sci.* **28** (1997) 67.
7. A. Salcido González, A.T. Celada Murillo, M.L. Díaz Flores, and A. Rodas Grapaín, *Un modelo de gases en redes para estimar la contribución de las emisiones de óxidos de nitrógeno de una planta termoeléctrica a la concentración de ozono en la atmósfera*. VIII Seminario de Especialidades Tecnológicas IIE-IMP-ININ, Morelos (1996).
8. G.P. Georgopoulos and J.H. Seinfeld. *Atmos. Environ.* **20** (1986) 1809.
9. M.Z. Jacobson. *J. Geoph. Res*. **108** (2003)AAC 4-1.
10. A. Prakash, A.P. Bapat, and M.R. Zachariah, *Aerosol Sci. and Technol.* **37** (2003) 892.
11. L.I. Zaichik and A.L. Solov'ev, *High Temperature* **40** (2002) 422.
12. M.Z. Jacobson, *Atmos. Environ*. **31A** (1997) 131.
13. F. Gelbard and J.H. Seinfeld, *Journal of Colloid and Interface Science* 68 (1979) 363.
14. M.Z. Jacobson, *Developing, coupling, and applying a gas, aerosol, transport, and radiation model to study urban and regional air pollution*. Ph. D. Thesis, Dept. of Atmospheric Sciences, University of California, USA, (1994) 436.
15. A.T. Celada and A. Salcido, *Rev. Mex. Fís.***51** (2005) 379.
16. A.T. Celada and A. Salcido, *Journal of Aerosol Sci.* **1** (2003) S337.
17. A.T. Celada, *Modelación del proceso de coagulación en plumas de fuentes fijas,* PH D Thesis, Departamento de Ing. Mecánica, Centro Nacional de Investigación y Desarrollo Tecnológico, México (2006) 120.
18. A. Salcido, A.T. Celada, M.L. Díaz, and A. Rodas. *Modelación matemática de plumas reactivas*. Proceedings Mexico Power 96 Conference. Monterrey, Nuevo León, (1996).
19. A. Rodas Grapaín, Modelación matemática y numérica de la dispersión turbulenta de plumas de contaminantes reactivos. M Sc Thesis. División de Estudios de Posgrado de la Facultad de Química. Universidad Nacional Autónoma de México. México D.F. (1999).
20. A. Rodas Grapaín and A. Salcido González, *Tecnología, Ciencia, Educación. Instituto Mexicano de Ingenieros Químicos* **15** (2000) 61.
21. Y. Zhu, W.C. Hinds, S. Kim, and C. Sioutas. *Journal of the Air & Waste Management Association* **52** (2002) 1032.
22. Y. Zhu, W.C. Hinds, S. Kim, S. Shen, and C. Siuotas, *Atmospheric Environment* **36** (2002) 4323.
23. E.P. Weijers, G.P.A. Kos, and P.A.C. Jongejan, *Ultrafine particle emissions along motorways. Emission factors, concentrations and size distributions*, Report No. ECN-C-003-041, Energy Research Centre of the Netherlands (ECN),(2003)41.
24. A. Salcido *et al.*, *Il Nuovo Cimento*, **26**(2003)317.
25. M.Z. Jacobson, *Fundamentals of Atmospheric Modeling* (Cambridge University Press. Cambridge, UK, 1999) p. 656.
26. A.T. Celada and A. Salcido, *Coagulation and atmospheric dispersion of polydisperse aerosols,* Proc. of The Second IASTED International Conference on Environmental Modelling and Simulation 2006, Saint Thomas, Virgin Islands, E.U.A., (2006)48.
27. D.S. Kim, S.H. Park, Y.M. Song, D.H. Kim, and K.W. Lee, *J. Aerosol Sci.* **34** (2003) 859.
28. S.J. Rooker, *J. Aerosol Sci.* **10** (1979) 139.
29. K. Okuyama, Y. Kousaka, Y. Kida, and T. Yoshida, *J. Chem. Eng. Japan* **10** (1977) 142.
30. F.E. Kruis and K.A. Kusters, *Chem. Eng. Commun*. **158** (1997) 201.